Synchronization of the fractional-order generalized augmented Lü system and its circuit implementation*

Xue Wei(薛 薇)[a)†], Xu Jin-Kang(徐进康)[a)], Cang Shi-Jian(仓诗建)[b)], and Jia Hong-Yan(贾红艳)[a)]

[a)] Department of Automation, Tianjin University of Science and Technology, Tianjin 300222, China
[b)] Department of Industry Design, Tianjin University of Science and Technology, Tianjin 300222, China

(Received 9 September 2013; revised manuscript received 16 December 2013; published online 10 April 2014)

In this paper, the synchronization of the fractional-order generalized augmented Lü system is investigated. Based on the predictor–corrector method, we obtain phase portraits, bifurcation diagrams, Lyapunov exponent spectra, and Poincaré maps of the fractional-order system and find that a four-wing chaotic attractor exists in the system when the system parameters change within certain ranges. Further, by varying the system parameters, rich dynamical behaviors occur in the 2.7-order system. According to the stability theory of a fractional-order linear system, and adopting the linearization by feedback method, we have designed a nonlinear feedback controller in our theoretical analysis to implement the synchronization of the drive system with the response system. In addition, the synchronization is also shown by an electronic circuit implementation for the 2.7-order system. The obtained experiment results accord with the theoretical analyses, which further demonstrate the feasibility and effectiveness of the proposed synchronization scheme.

Keywords: fractional-order generalized augmented Lü system, nonlinear feedback synchronization, numerical simulation, circuit design

PACS: 05.45.–a, 05.45.Pq **DOI:** 10.1088/1674-1056/23/6/060501

1. Introduction

Currently, many synchronization approaches of the fractional-order chaotic system have been proposed, such as active control,[1] linearization by feedback,[2] sliding mode control,[3,4] adaptive control,[5] impulse control,[6] passive control,[7] lag synchronization,[8] and projective synchronization.[9,10]

By introducing a simple linear state feedback controller into the third-order equation of differential equations of the augmented Lü system,[11] in 2009 a new three-dimensional (3D) autonomous system was proposed in Ref. [12], namely the generalized augmented Lü system. The new system can generate a real four-wing fan-shaped chaotic attractor without any external excitation. On the basis of Ref. [12], the synchronization of the fractional-order generalized augmented Lü system is investigated in this paper. It is found by analyzing phase portraits, bifurcation diagrams, Lyapunov exponent spectra, and Poincaré maps of the fractional-order generalized augmented Lü system that a four-wing chaotic attractor exists in the new system when the system parameters change within certain ranges. According to the predictor–corrector method, by the numerical simulations of the 2.7-order generalized augmented Lü system, we find that the system presents rich dynamical characteristics, including four-wing chaotic attractors, periodic attractors, and quasi-periodic attractors. On this basis, with the nonlinear feedback method, a synchronous controller is designed to convert the nonlinear error system of chaotic synchronization into a linear error system, and the synchronization of the fractional-order generalized augmented Lü system is realized according to the stability theory of a fractional-order linear system. In addition, utilizing the modularization method to design analog circuits, the synchronization of the fractional-order chaotic system in Multisim is also obtained. The obtained experiment results accord with the theoretical analyses, which can further demonstrate the feasibility and effectiveness of the proposed control scheme.

2. Synchronization of fractional-order generalized augmented Lü system

2.1. Mathematic model of system and problem description

The mathematical model of fractional-order chaotic system can be described as follows:

$$\frac{\mathrm{d}^q \boldsymbol{x}}{\mathrm{d}t^q} = A\boldsymbol{x} + f(\boldsymbol{x}), \tag{1}$$

where $0 < q < 1$, $A \in R^{n\times n}$ is the matrix of system parameters, $\boldsymbol{x} = (x_1, x_2, \ldots, x_n)^{\mathrm{T}} \in R^n$ is the state vector of system (1), $f(\boldsymbol{x}) = (f_1(x), f_2(x), \ldots, f_n(x))^{\mathrm{T}} \in R^{n\times 1}$ is the nonlinear term. System (1) is considered to be the drive system, and the response system is as follows:

$$\frac{\mathrm{d}^q \boldsymbol{y}}{\mathrm{d}t^q} = B\boldsymbol{y} + g(\boldsymbol{y}) + \boldsymbol{u}, \tag{2}$$

*Project supported by the National Natural Science Foundation of China (Grant No. 61174094) and the Young Scientists Fund of the National Natural Science Foundation of China (Grant No. 11202148).

†Corresponding author. E-mail: xuewei@tust.edu.cn

© 2014 Chinese Physical Society and IOP Publishing Ltd

where $0 < q < 1$, $B \in R^{n\times n}$ is the matrix of system parameters, $\boldsymbol{y} = (y_1, y_2, \ldots, y_n)^{\mathrm{T}} \in R^n$ is the state vector of system (2), $g(\boldsymbol{y}) = (g_1(y), g_2(y), \ldots, g_n(y))^{\mathrm{T}} \in R^{n\times 1}$ is the nonlinear term, and $\boldsymbol{u} = (u_1, u_2, \ldots, u_n)^{\mathrm{T}}$ is the controller.

From the drive system (1) and the response system (2), the state error vector is obtained which can be expressed as $\boldsymbol{e} = \boldsymbol{y} - \boldsymbol{x} = (e_1, e_2, \ldots, e_n)^{\mathrm{T}}$, and we should design the appropriate controller $\boldsymbol{u}$ to make $\lim\limits_{t\to\infty} \boldsymbol{e} = 0$.

According to Ref. [12], we investigate the commensurate fractional-order generalized augmented Lü system in this paper and its mathematical model is as follows:

$$\begin{cases} \dfrac{\mathrm{d}^q x_1}{\mathrm{d}t^q} = -\dfrac{ab}{a+b}x_1 - x_2x_3, \\ \dfrac{\mathrm{d}^q x_2}{\mathrm{d}t^q} = ax_2 + x_1x_3, \\ \dfrac{\mathrm{d}^q x_3}{\mathrm{d}t^q} = bx_3 + x_1x_2 + cx_1, \end{cases} \tag{3}$$

where $0 < q < 1$, a, b, and c are constants, $a < 0$ and $b < 0$.

If system (3) is considered as the drive system, the relevant response system is as follows:

$$\begin{cases} \dfrac{\mathrm{d}^q y_1}{\mathrm{d}t^q} = -\dfrac{ab}{a+b}y_1 - y_2y_3 + u_1, \\ \dfrac{\mathrm{d}^q y_2}{\mathrm{d}t^q} = ay_2 + y_1y_3 + u_2, \\ \dfrac{\mathrm{d}^q y_3}{\mathrm{d}t^q} = by_3 + y_1y_2 + cy_1 + u_3. \end{cases} \tag{4}$$

In order to synchronize the chaotic systems that are in different initial conditions, the target is to choose the appropriate controllers u_1, u_2, and u_3.

2.2. Design of synchronization controller

Lemma 1[13] Consider the following fractional-order linear system: $\mathrm{d}^q\boldsymbol{x}/\mathrm{d}t^q = C\boldsymbol{x}$, where $0 < q < 1$, $\boldsymbol{x} = (x_1, x_2, \ldots, x_n)^{\mathrm{T}} \in R^n$, and $C \in R^{n\times n}$. If $|\arg(\lambda_i)| > q\pi/2$, where λ_i $(i = 1, 2, 3)$ are eigenvalues of C, then the asymptotical stability of the origin of the fractional-order system, that is, $\lim\limits_{t\to\infty} \boldsymbol{x} = 0$, is reached.

The drive system (3) is written in the form of system (1), as follows:

$$\frac{\mathrm{d}^q\boldsymbol{x}}{\mathrm{d}t^q} = \begin{pmatrix} -\dfrac{ab}{a+b} & 0 & 0 \\ 0 & a & 0 \\ c & 0 & b \end{pmatrix}\boldsymbol{x} + \begin{pmatrix} -x_2x_3 \\ x_1x_3 \\ x_1x_2 \end{pmatrix}. \tag{5}$$

Then, the response system (4) can be described as system (2) in the form of

$$\frac{\mathrm{d}^q\boldsymbol{y}}{\mathrm{d}t^q} = \begin{pmatrix} -\dfrac{ab}{a+b} & 0 & 0 \\ 0 & a & 0 \\ c & 0 & b \end{pmatrix}\boldsymbol{y} + \begin{pmatrix} -y_2y_3 \\ y_1y_3 \\ y_1y_2 \end{pmatrix} + \boldsymbol{u}. \tag{6}$$

Here, we adopt the linearization by feedback method[2] to realize the synchronization of the fractional-order generalized augmented Lü system by selecting $\boldsymbol{u} = f(\boldsymbol{x}) - g(\boldsymbol{y}) - K\boldsymbol{e}$ as the controller

$$\boldsymbol{u} = f(\boldsymbol{x}) - g(\boldsymbol{y}) - K\boldsymbol{e} = \begin{pmatrix} -x_2x_3 \\ x_1x_3 \\ x_1x_2 \end{pmatrix} - \begin{pmatrix} -y_2y_3 \\ y_1y_3 \\ y_1y_2 \end{pmatrix} - K\boldsymbol{e},$$

where $\boldsymbol{e} = \boldsymbol{y} - \boldsymbol{x} = (e_1, e_2, e_3)^{\mathrm{T}}$.

From Eqs. (5), (6), and $\boldsymbol{u}$, we can obtain the error system as follows:

$$\frac{\mathrm{d}^q e}{\mathrm{d}t^q} = \begin{pmatrix} -\dfrac{ab}{a+b} & 0 & 0 \\ 0 & a & 0 \\ c & 0 & b \end{pmatrix}\boldsymbol{e} - K\boldsymbol{e}. \tag{7}$$

Let

$$K = \begin{pmatrix} 1 - \dfrac{ab}{a+b} & 0 & 0 \\ 0 & 0 & 0 \\ 0 & 0 & 0 \end{pmatrix},$$

so the error system will be $\dfrac{\mathrm{d}^q e}{\mathrm{d}t^q} = \begin{pmatrix} -1 & 0 & 0 \\ 0 & a & 0 \\ c & 0 & b \end{pmatrix}\boldsymbol{e} = C\boldsymbol{e}$.

By calculating the equation of the error system, the eigenvalues of C are, $\lambda_1 = -1, \lambda_2 = a$, and $\lambda_3 = b$ because $a < 0$ and $b < 0$, all eigenvalues λ_i $(i = 1, 2, 3)$ are negative, namely $|\arg(\lambda_i)| = \pi > q\pi/2$. According to Lemma 1, the asymptotical stability of the origin of the error system, that is $\lim\limits_{t\to\infty} e = 0$, is reached, achieving the goal of synchronizing the fractional-order generalized augmented Lü system.

3. Model and basic dynamical characteristic analysis

As is well known, the mathematical model of the commensurate fractional-order generalized augmented Lü system is as follows:

$$\begin{cases} \dfrac{\mathrm{d}^q x_1}{\mathrm{d}t^q} = -\dfrac{ab}{a+b}x_1 - x_2x_3, \\ \dfrac{\mathrm{d}^q x_2}{\mathrm{d}t^q} = ax_2 + x_1x_3, \\ \dfrac{\mathrm{d}^q x_3}{\mathrm{d}t^q} = bx_3 + x_1x_2 + cx_1, \end{cases} \tag{8}$$

where $0 < q < 1$, a, b, and c are constants, $a < 0$ and $b < 0$. Generally, the order of a system is considered as the sum of each order of its equation. For example, for system (3), it is considered to be the 2.7-order system when $q = 0.9$. Above all, to analyze the influence of fractional order q on system (3) with $a = -10, b = -5$, and $c = 0.5$, we draw the bifurcation diagram of system (3) in Fig. 1 when q changes within $[0.65,\ 1]$.

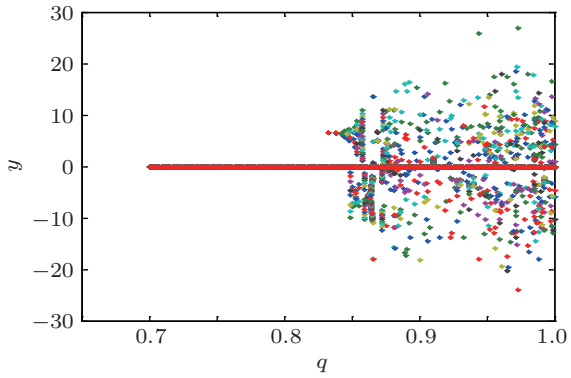


Fig. 1. (color online) Bifurcation diagram of system (3) with $a = -10$, $b = -5$, and $c = 0.5$ when $q \in [0.65,\ 1]$.

From Fig. 1, we can see that the fractional-order generalized augmented Lü system can still presents chaos when $q \in [0.85,\ 1]$ and the system will be periodic or even in a stable state when $q < 0.85$. For system (3), since the phenomenon of chaos is obvious when $q = 0.9$ and it is also convenient for us to implement it from physical level when designing the circuit, we will concentrate on the 2.7-order system in the following part. By utilizing the predictor–corrector method, we obtain the attractors of system (3) when $q = 0.9$, $a = -10$, $b = -5$, and $c = 0.5$, The phase portraits are depicted in Fig. 2.

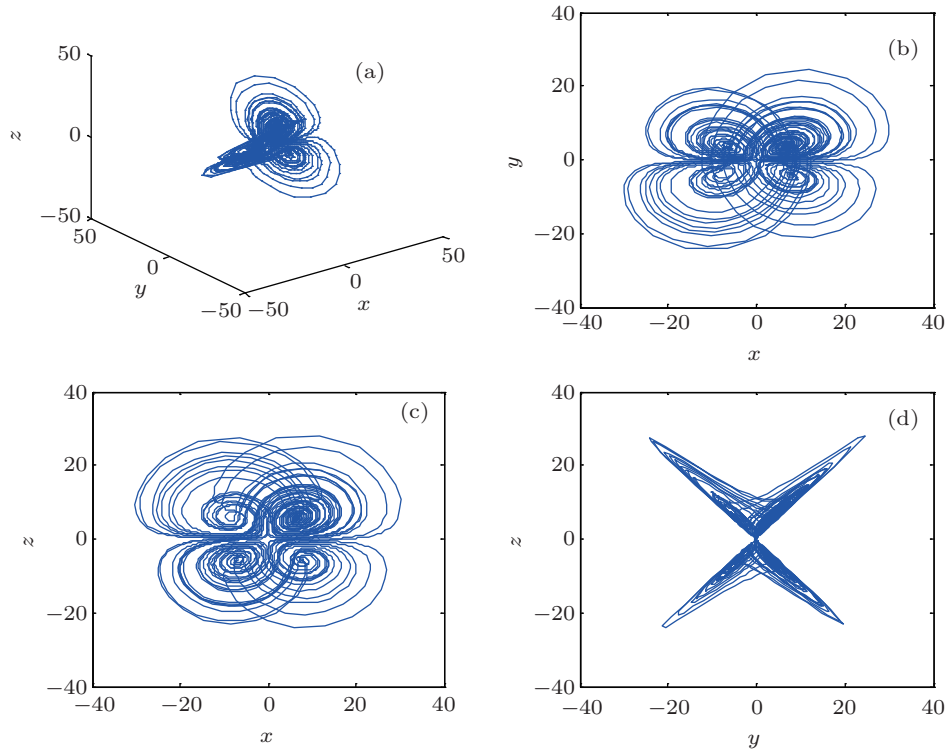


Fig. 2. (color online) (a) Phase portraits of system (3) with $q = 0.9$, $a = -10$, $b = -5$, and $c = 0.5$; (b) x_1–x_2 plan; (c) $1 - x_3$ plan; (d) x_2–x_3 plan.

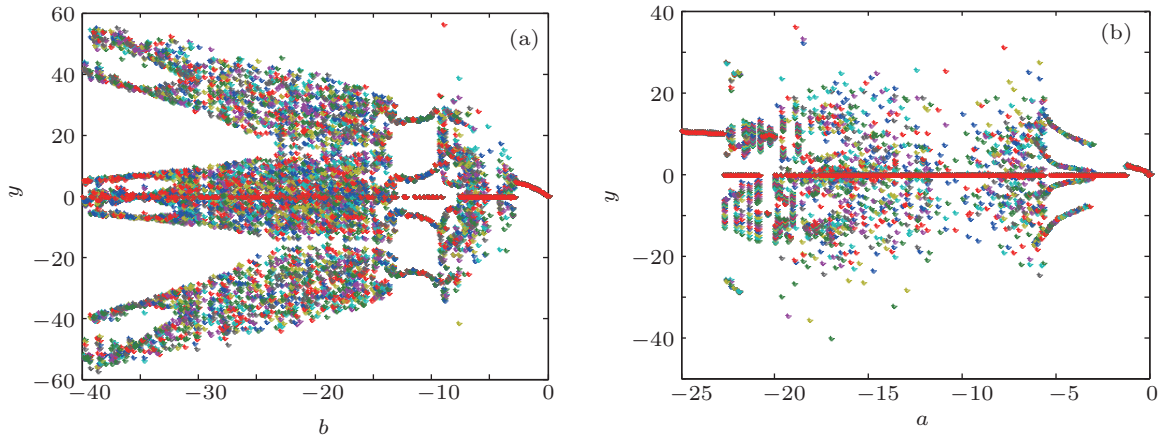


Fig. 3. (color online) Bifurcation diagrams of system (3) on y axis: (a) $q = 0.9$, $a = -10$, $c = 0.5$, $b \in [-40,\ 0]$; (b) $q = 0.9$, $b = -5$, $c = 0.5$, $a \in [-25,\ 0]$.

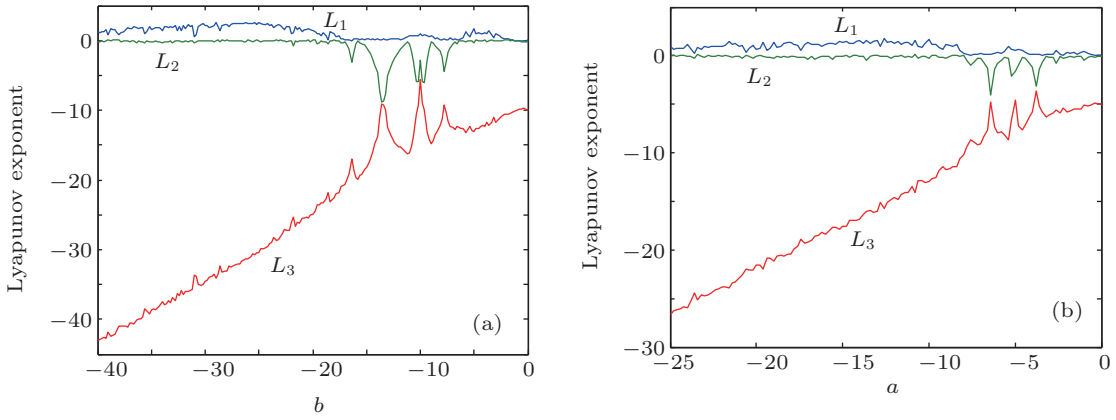


Fig. 4. (color online) Lyapunov exponent diagrams of system (3): (a) $q = 0.9$, $a = -10$, $c = 0.5$, $b \in [-40,\ 0]$; (b) $q = 0.9$, $b = -5$, $c = 0.5$, $a \in [-25,\ 0]$.

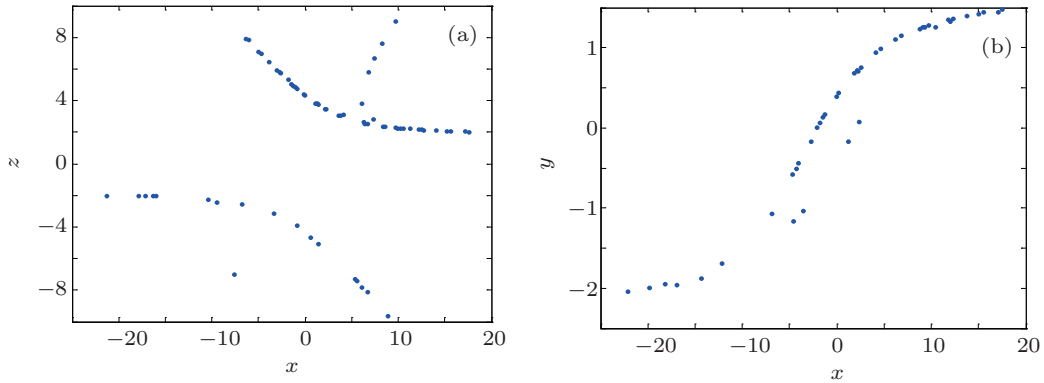


Fig. 5. (color online) Poincaré section maps of system (3) with $q = 0.9$, $a = -10$, $b = -5$, and $c = 0.5$, (a) section of $y = 1.5$, (b) section of $z = 2$.

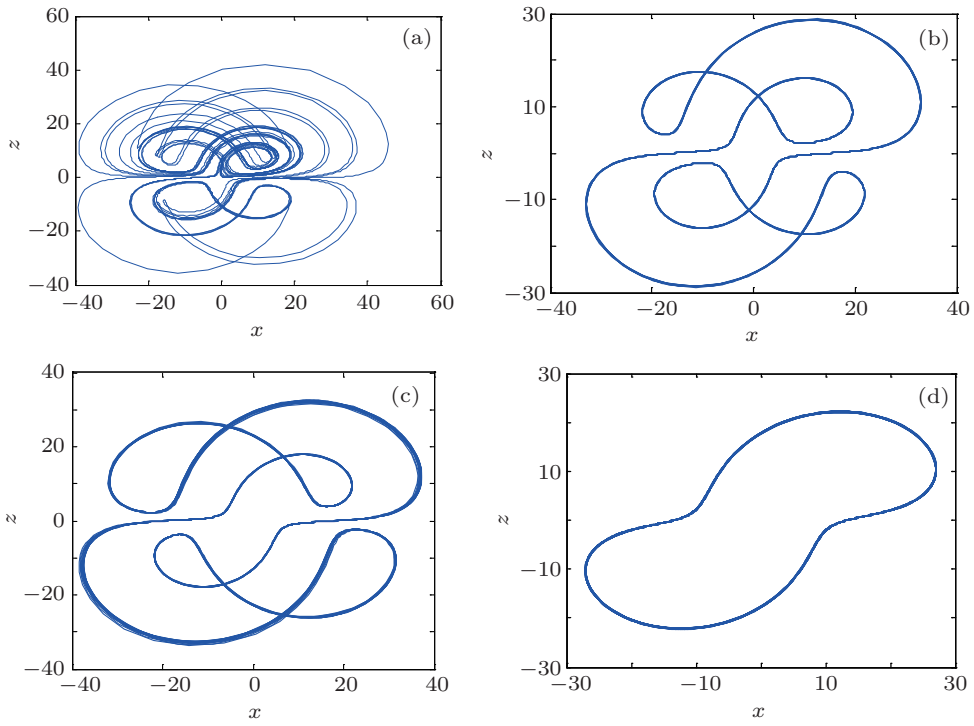


Fig. 6. (color online) x_1–x_3 plan phase portraits of system (3) with $q = 0.9$, $a = -10$, $c = 0.5$, $b = -7$, -8, -9, -10; (a) x_1–x_3 plan of $b = -7$; (b) x_1–x_3 plan of $b = -8$; (c) x_1–x_3 plan of $b = -9$; (d) x_1–x_3 plan of $b = -10$;

From the phase portraits shown in Fig. 2, we can see that there exist chaotic attractors in system (3) with $q = 0.9$, $a = -10$, $b = -5$, and $c = 0.5$. Furthermore, for the 2.7-order generalized augmented Lü system, the bifurcation diagrams and the Lyapunov exponent spectra are shown in Fig. 3 and Fig. 4, respectively, where L_1, L_2, and L_3 are Lyapunove exponents of the system (3). From bifurcation diagrams and Lyapunov exponent spectra, we can observe that Lyapunov exponent spectra give results that are completely consistent with the bifurcation diagrams. In a large range of parameters a and b, bifurcation diagrams in Fig. 3 show that there exist abundant and complex dynamical behaviors in the 2.7-order system, and we can see that the system has one positive Lyapunov exponent and presents a chaotic state from Fig. 4.

In addition, we draw the Poincaré maps of system (3) when $q = 0.9$, $a = -10$, $b = -5$, and $c = 0.5$ at the section of $y = 1.5$ and $z = 2$ as shown in Fig. 5. We can find that the 2.7-order system is chaotic and its attractor has a four-wing fan-shaped structure from the Poincaré maps in Fig. 5.

With the variation of parameters in system (3), the stability of the equilibrium point of the system changes and the state of system also changes. When $q = 0.9$, $a = -10$, $c = 0.5$, and $b = -7$, -8, -9, -10, different dynamical behaviors, such as chaotic orbits, periodic orbits, and quasi-periodic orbits are present in system (3), respectively. The simulation results are shown in Fig. 6.

4. Numerical simulation

Here, taking the 2.7-order generalized augmented Lü system as an example, we conduct the numerical simulation of the synchronization via Matlab. When the system parameters are chosen to be $q = 0.9$, $a = -10$, $b = -5$, and $c = 0.5$, in time steps of 0.01, with the initial values of the state variables being $x_1(0) = 0.1$, $x_2(0) = 0.1$, $x_3(0) = 0.1$, $y_1(0) = 3$, $y_2(0) = 4$, $y_3(0) = 5$, respectively, we can observe that the drive system and the response system are in asymptotic synchronization from Fig. 7.

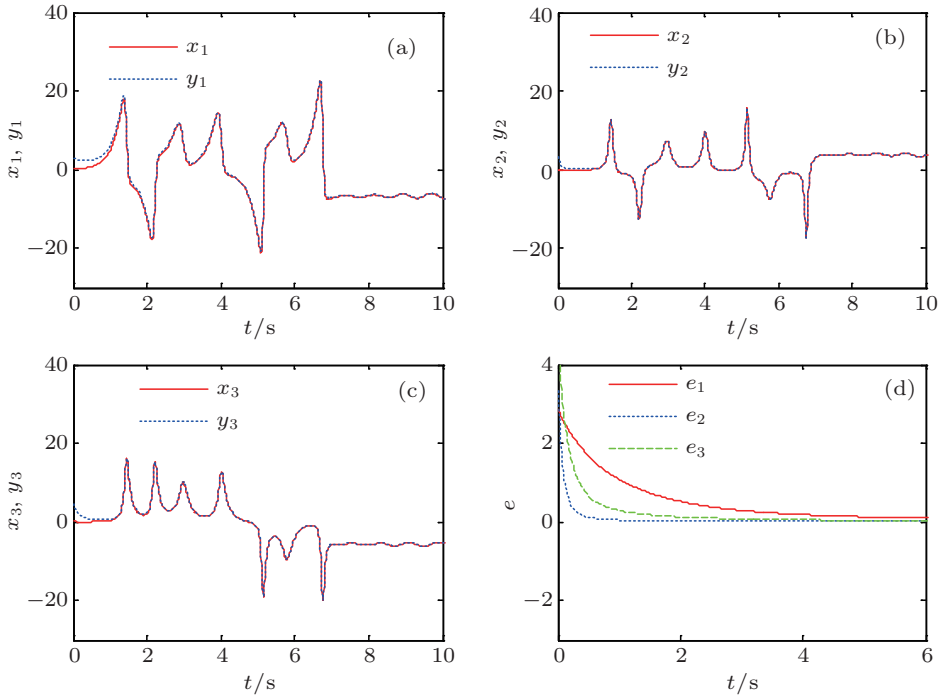


Fig. 7. (color online) (a) Variation of (x_1, y_1) with time; (b) variation of (x_2, y_2) with time; (c) variation of (x_3, y_3) with time; (d) the synchronization errors versus time t.

5. Circuit design for the 2.7-order generalized augmented Lü system

Because fractional calculus does not allow the direct calculation of the differential operators in time domain, we usually adopt the method of approximation conversion from time domain to frequency domain to design a circuit. Based on Bode diagrams, Ahmad and Sprott[14] deduced $1/s^q$ ($q = 0.1 \sim 0.9$) with discrepancy 2 dB and 3 dB through linear approximation in frequency domain. Here, we utilize the approximation of $1/s^{0.9}$ with discrepancy 2 dB to design the analog circuit. According to Ref. [14], we can obtain

$$\frac{1}{s^{0.9}} \approx \frac{2.2675(s+1.292)(s+215.4)}{(s+0.01292)(s+215.4)(s+359.4)}.$$

A circuit design where resistors and capacitors are connected in parallel was proposed in Ref. [15] to realize fractional calculus. When $q = 0.9$, the circuit unit is designed

as shown in Fig. 8, where $R_1 = 62.84$ MΩ, $R_2 = 250$ kΩ, $R_3 = 2.5$ kΩ; $C_1 = 1.232$ μF, $C_2 = 1.84$ μF, and $C_3 = 1.1$ μF.

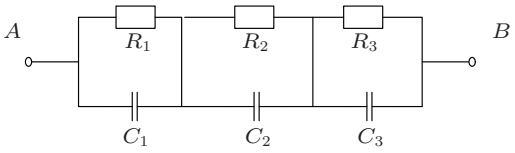


Fig. 8. Circuit unit of $1/s^{0.9}$.

We select LF353P as the amplifier and AD633JN (the output gain is 0.1) as the multiplier to design the synchronous circuit. The module design schematic plot of the synchronization for the 2.7-order system is shown in Fig. 9. In order to restrict the change of state variables to the operating voltage of the analog circuit, the state variables are reduced by 20 times, namely let $(x_1, x_2, x_3) \to (20x_1, 20x_2, 20x_3)$ and $(y_1, y_2, y_3) \to (20y_1, 20y_2, 20y_3)$.

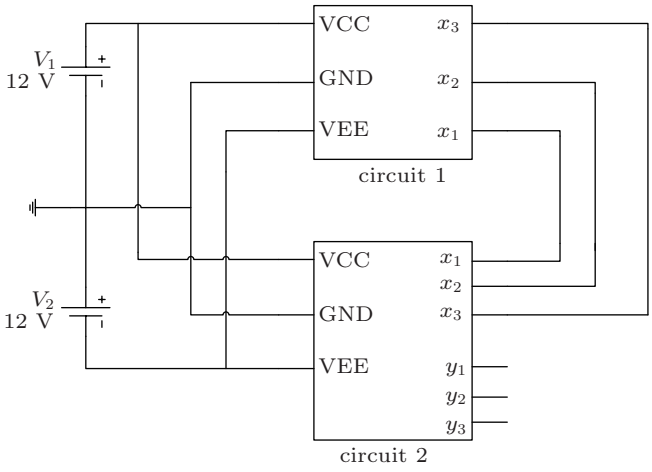


Fig. 9. Module circuit of the 2.7-order generalized augmented Lü system.

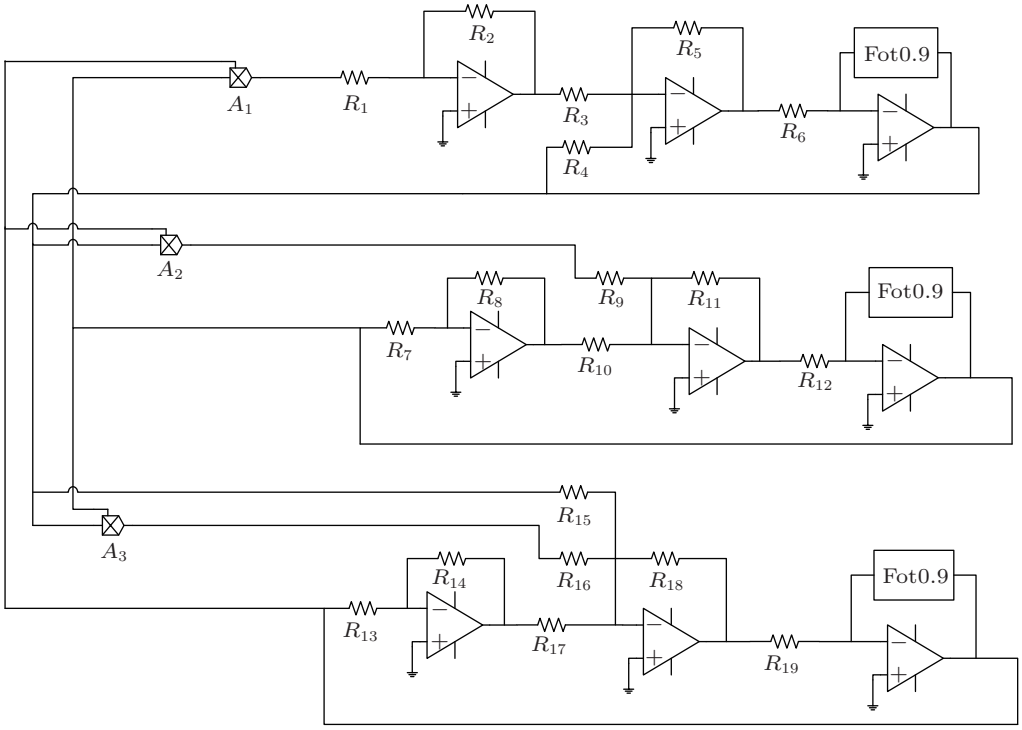


Fig. 10. Circuit diagram of system (3) when $q = 0.9$.

When $q = 0.9$, $a = -10$, $b = -5$, and $c = 0.5$, the circuit schematics of the drive system (3) and the response system (4) which correspond to circuit 1 and circuit 2 in Fig. 9 are given, respectively, in Figs. 10 and 11, where $R_{23} = 23.1$ kΩ, $R_4 = 30$ kΩ, R_7, $R_{27} = 10$ kΩ, R_{15}, $R_{35} = 200$ kΩ, R_1, R_9, R_{16}, R_{20}, R_{29}, $R_{36} = 500$ Ω, R_2, R_3, R_5, R_8, R_{10}, R_{11}, R_{14}, R_{17}, R_{18}, R_{21}, R_{22}, R_{24}, R_{25}, R_{28}, R_{30}, R_{31}, R_{34}, R_{37}, $R_{38} = 100$ kΩ, R_6, R_{12}, R_{13}, R_{19}, R_{26}, R_{32}, R_{33}, $R_{39} = 20$ kΩ.

For the drive system, the circuit equation is as follows:

$$\begin{cases} \dfrac{\mathrm{d}^{0.9}x_1}{\mathrm{d}t^{0.9}} = \dfrac{R_5}{R_4R_6}x_1 - \dfrac{R_2R_5}{R_1R_3R_6}(0.1x_2x_3), \\ \dfrac{\mathrm{d}^{0.9}x_2}{\mathrm{d}t^{0.9}} = -\dfrac{R_8R_{11}}{R_7R_{10}R_{12}}x_2 + \dfrac{R_{11}}{R_9R_{12}}(0.1x_1x_3), \\ \dfrac{\mathrm{d}^{0.9}x_3}{\mathrm{d}t^{0.9}} = -\dfrac{R_{14}R_{18}}{R_{13}R_{17}R_{19}}x_3 + \dfrac{R_{18}}{R_{16}R_{19}}(0.1x_1x_2) \\ \qquad\qquad + \dfrac{R_{18}}{R_{15}R_{19}}x_1. \end{cases} \tag{9}$$

The circuit equation of the response system is as follows:

$$\begin{cases} \dfrac{\mathrm{d}^{0.9}y_1}{\mathrm{d}t^{0.9}} = -\dfrac{R_{23}R_{25}}{R_{21}R_{24}R_{26}}y_1 - \dfrac{R_{23}R_{25}}{R_{20}R_{24}R_{26}}(0.1x_2x_3) \\ \qquad\qquad + \dfrac{R_{25}}{R_{22}R_{26}}x_1, \\ \dfrac{\mathrm{d}^{0.9}y_2}{\mathrm{d}t^{0.9}} = -\dfrac{R_{28}R_{31}}{R_{27}R_{30}R_{32}}y_2 + \dfrac{R_{31}}{R_{29}R_{32}}(0.1x_1x_3), \\ \dfrac{\mathrm{d}^{0.9}y_3}{\mathrm{d}t^{0.9}} = -\dfrac{R_{34}R_{38}}{R_{33}R_{37}R_{39}}y_3 + \dfrac{R_{38}}{R_{36}R_{39}}(0.1x_1x_2) \\ \qquad\qquad + \dfrac{R_{38}}{R_{35}R_{39}}y_1. \end{cases} \tag{10}$$

We can change the values of a, b, c, and $ab/(a+b)$ by adjusting R_7, R_{13}, R_{15}, and R_4 of circuit diagram in Fig. 10, while values of R_{27}, R_{33}, R_{35}, and R_{22} of the circuit diagram in Fig. 11 correspond to the value of a, b, c, and $ab/(a+b)$, Fot0.9 module represents 0.9-order circuit unit shown in Fig. 8.

The circuit simulation result of the 2.7-order generalized augmented Lü system in Fig. 10 is shown in Fig. 12, we observed that the system is in a chaotic state. Moreover, we build an analog circuit and the circuit implementation result that is shown in Fig. 13 through the oscilloscope TDS2014B is consistent with the simulation result. In addition, we obtain the curve of state variables x_2 and y_2 as shown in Fig. 14 through the circuit simulation, and we can observe that the curve is a straight line through the origin and $x_2 = y_2$ from Fig. 14, indicating that x_2 and y_2 achieve synchronization completely, and we also obtained the circuit experiment diagram of the x_2–y_2 plan through the oscilloscope TDS2014B as shown in Fig.15, which is in accordance with the circuit simulation result.

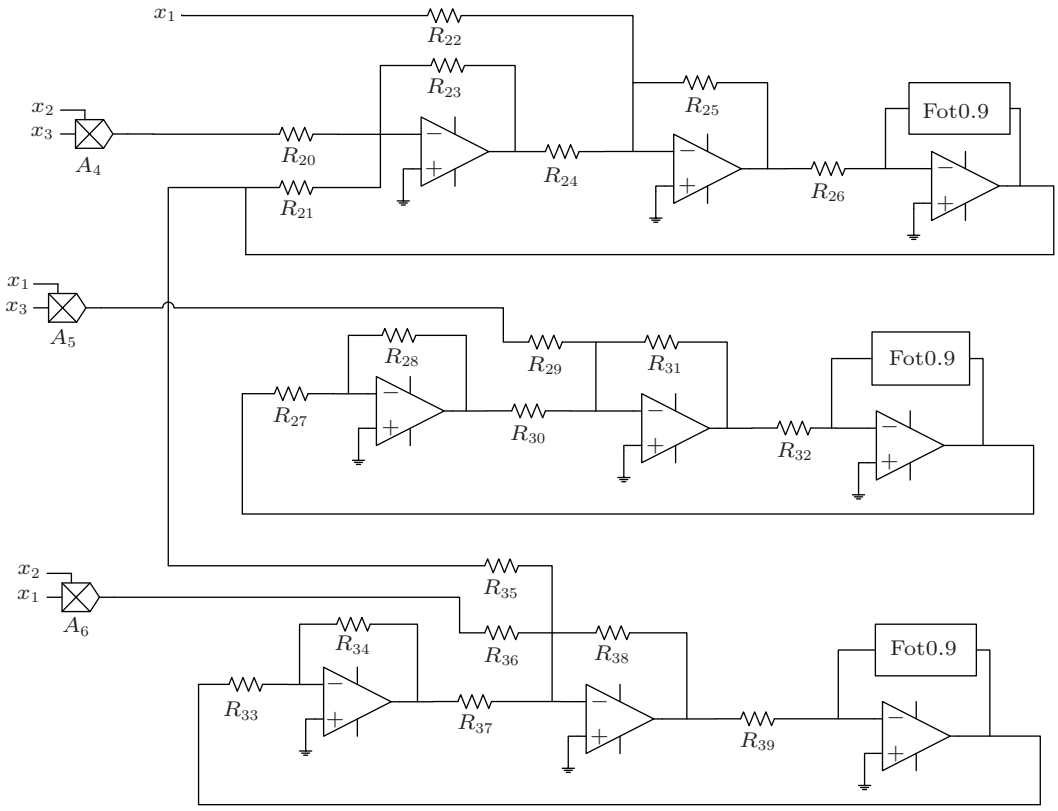


Fig. 11. Circuit diagram of system (4) when $q = 0.9$.

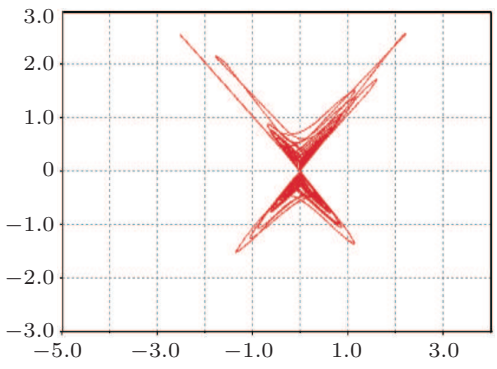


Fig. 12. (color online) Circuit simulation diagram of x_2–x_3 plan of the 2.7-order drive system (3).

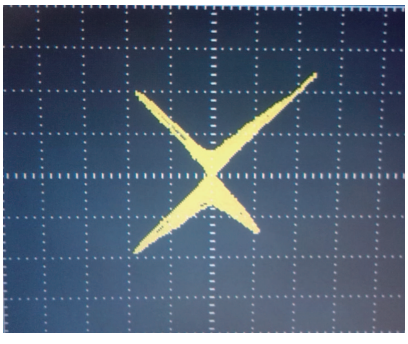


Fig. 13. (color online) Circuit experiment diagram of x_2–x_3 plan of the 2.7-order drive system (3) from the oscilloscope TDS2014B.

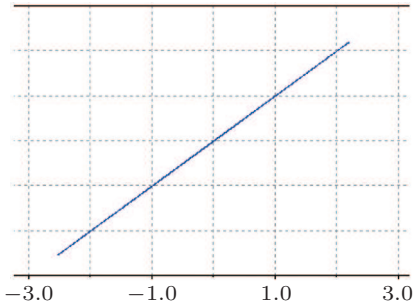


Fig. 14. (color online) Circuit simulation diagram of x_2–y_2 plan.

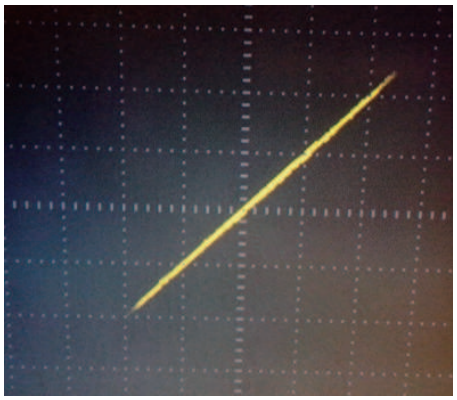


Fig. 15. (color online) Circuit experiment diagram of x_2–y_2 plan from the oscilloscope TDS2014B.

6. Conclusion

In this paper, we have investigated the commensurate fractional-order generalized augmented Lü system. By analyzing phase portraits, bifurcation diagrams, Lyapunov exponent spectra, and Poincaré maps of fractional-order generalized augmented Lü system, we find that the system presents chaos within a certain range of parameters. With the change of the system parameters, the 2.7-order system will be in different states such as four-wing chaos, period, quasi-period, indicating that there are abundant dynamical behaviors in the fractional-order chaotic system. Moreover, the synchronization problem of the fractional-order generalized augmented Lü system was investigated. We designed the synchronous controller to achieve synchronization between the drive system and the response system according to the linearization by feedback method and have proved the synchronous controller to be correct through the stability theory of fractional-order linear system. On this basis, the electronic circuit for the synchronization of the 2.7-order chaotic systems was designed to implement the system, and the circuit experiment results accord well with the theoretical analyses and the numerical simulation results, verifying the effectiveness and feasibility of the method and providing theoretical basis and technique support for the further application and research of the fractional-order chaotic system.

References

[1] Li G H 2005 *Chin. Phys.* **14** 472
[2] Zhang R X and Yang S P 2008 *Acta Phys. Sin.* **57** 6852 (in Chinese)
[3] Qi D L, Wang Q and Yang J 2011 *Chin. Phys. B* **20** 100505
[4] Li M and Liu C X 2010 *Chin. Phys. B* **19** 100504
[5] Zhang R X and Yang S P 2011 *Nonlinear Dyn.* **66** 831
[6] Wang X Y, Zhang Y L, Lin D and Zhang N 2011 *Chin. Phys. B* **20** 030506
[7] Wu C J, Zhang Y B and Yang N N 2011 *Chin. Phys. B* **20** 060505
[8] Zhang R X and Yang S P 2011 *Chin. Phys. B* **20** 090512
[9] Liu L, Liang D L and Liu C X 2012 *Nonlinear Dyn.* **69** 1929
[10] Huang L L and Ma N 2012 *Acta Phys. Sin.* **61** 160510 (in Chinese)
[11] L J H, Chen G R and Cheng D Z 2004 *Int. J. Bifur. Chaos* **14** 1507
[12] Qiao X H and Bao B C 2009 *Acta Phys. Sin.* **58** 8152 (in Chinese)
[13] Matignon D 1996 in: *IMACS, IEEE-SMC,* Lille, France 963
[14] Ahmad W M, and Sprott J C 2003 *Chaos, Solitons & Fractals* **16** 339
[15] Wang Z and Sun W 2012 *Computer Engineering & Science* **34** 187